Sound & Vibration 2025, 59(6), 3284.
doi: https://doi.org/10.59400/sv3284

Article

Dual-idler gear-rack transmission mechanism: Analysis and optimization of vibration excited by defects

Wenhe Han[1,2], Pengfei Wang[3], Shuming Guo[3], Shuyan Wang[3,*], Chenglin Ruan[3], Jiahao Yuan[3]

[1] Science and Technology Development Co., Ltd. of Shanghai Research Institute of Building Sciences, Shanghai 201506, China

[2] Shanghai Engineering Research Center for Safety Intelligent Control of Building Machinery, Shanghai 200032, China

[3] College of Mechanical Engineering, Donghua University, Shanghai 201620, China

*** Corresponding author:** Shuyan Wang, shuyan@dhu.edu.cn

CITATION

Han W, Wang P, Guo S, et al. Dual-idler gear-rack transmission mechanism: Analysis and optimization of vibration excited by defects. Sound & Vibration. 2025; 59(6): 3284. https://doi.org/10.59400/sv3284

ARTICLE INFO

Received: 24 August 2025
Revised: 21 October 2025
Accepted: 28 October 2025
Available online: 10 November 2025

Abstract: In long-distance heavy-load transmission systems, the unique high load-bearing capacity and trajectory constraint characteristics of the double-idler rack-and-pinion mechanism can significantly improve the reliability of the transmission system. However, engineering practice has revealed that factors such as tooth profile distortion caused by residual stress from rack rolling, flatness errors of mounting surfaces, and linear expansion due to environmental temperature changes can markedly alter the dynamic meshing characteristics of the rack and pinion. During the meshing process of the double-idler rack-and-pinion, the deformation of the rack and pinion and installation errors can lead to meshing impacts, thereby generating significant impact noise. This paper analyzes abnormal meshing states influenced by changes in center distance and pitch, constructs a defective meshing model for the rack and pinion, and further identifies factors more sensitive to defective meshing impacts through dynamic simulations. Finally, the paper proposes a flexible floating idler shaft structure that effectively reduces meshing impacts. The results demonstrate that the proposed structure yields significant improvements, particularly in the direction of pitch variation, which is more sensitive to vibrations. Specifically, the effective vibration values for random pitch micro-variations and sudden rack pitch changes are reduced by 60.5% and 23.4%, respectively, while those for sudden changes in rack center distance are reduced by 57.01%. This research provides new methodological support for optimizing the dynamic characteristics of precision rack-and-pinion transmission systems.

Keywords: dual-idler gear-rack mechanism; meshing impact; dynamic simulation; structural optimization; vibration and noise

1. Introduction

With the continuous improvement in industrial automation and the requirements for high-altitude working environments, fall arresters, as critical equipment ensuring the safety of workers, generate vibration and noise levels during operation that significantly affect the workers' mindset. The gear and rack, being the core of the fall arrester's transmission system, produce vibration and noise during the meshing process, which is the primary source of noise in the entire arrester mechanism. Conducting in-depth and professional analysis of the meshing vibration of the gear and rack not only helps reveal the intrinsic mechanisms of noise generation but also provides theoretical foundations and technical support for optimizing gear transmission design, reducing

vibration and noise, and enhancing the overall dynamic performance of the fall arrester. This significantly improves the safety of high-altitude operations and the reliability of the equipment [1].

Regarding the issues of gear meshing impact and vibration noise, scholars both domestically and internationally have conducted extensive research. Sun et al. [2] analyzed the influence of gear meshing impact caused by tooth wear on gear dynamic behavior. Zhang et al. [3] proposed a method that can be analyzed at the design stage for the vibration and noise problems of gearboxes. The correlation between gear parameters and noise is revealed by evaluating the influence of gear parameters on the root mean square value of gear tooth acceleration (linearly related to noise). Combined with the Simpack software dynamics model simulation and experimental data verification, this method can optimize gearbox design parameters, effectively reduce noise, and reduce later development costs. Liao et al. [4] proposed a new LOD-ICA fusion method for gearbox working noise signal acquisition, which can effectively separate the mixed signal components, complete the gearbox fault feature extraction, and enhance the fault diagnosability. Han et al. [5] examined the meshing characteristics of angular contact and broken-tooth fault spur gear pairs, providing an accurate model for judging the contact state of gear pairs. Tong et al. [6] proposed a new prediction model of gear meshing impact noise. By considering the coupling effect of lubricating oil and elastic tooth surface, the buffering mechanism of lubrication on impact noise is revealed. Xiong et al. [7] established a stiffness model and a friction coefficient model for metal-plastic gear pairs, explicitly considering the off-line meshing caused by significant elastic deformation. They validated the accuracy of the proposed friction model through theoretical calculation and experimental efficiency tests. Imin and Geni [8] used the SPH method to dynamically simulate the meshing impact process at different speeds, offering a new SPH-based numerical simulation algorithm for gear transmission design and optimization. https://www.tandfonline.com/author/Ning%2C+JieyuNing et al. [9] focused on the intensified driving gear-rack interactions experienced by rack vehicles on large mountain slopes. Addressing the limitations of treating racks as rigid bodies, they established a detailed dynamic model considering the vertical and longitudinal flexibilities of the rack using free beam and rod models. Validated by experimental data, the study analyzed the vibration and bending stress features under different mounting deviations. Additionally, Yang et al. [10] developed a rack-type vehicle-track coupled spatial dynamics model considering the dynamic effects of multi-stage gear transmission systems, grounded in typical vehicle-track coupled dynamics theory. Zhu et al. [11], considering the mechanism of meshing impact, established an improved nonlinear dynamics model for spur gear pairs that includes tooth backlash, contact ratio, multi-state meshing, and time-varying parameters. Geng et al. [12] studied how to reduce vibration in gear systems through active control technology, proposing a multi-channel VSMFxLMS algorithm based on the FxLMS algorithm and validating its effectiveness experimentally. Liu et al. [13] researched the mechanism of roller gear and involute rack meshing, demonstrating that the instantaneous velocity change during meshing is related to rack parameters. Ma et al. [14] proposed a Nonlinear Fast Kurtogram (NFK) method to address the

sensitivity of the traditional FK method to aperiodic shocks, successfully extracting gearbox fault features under strong shock interference. Dai et al. [15] proposed a hybrid analytic-computational (HAC) method for the nonlinear vibration analysis of spur gear pairs, which can accurately and efficiently predict the nonlinear dynamic response of gears. Wang et al. [16] constructed a series of suitable models to analyze the influence mechanism of pitch deviation on the meshing stiffness and vibration noise of helical cylindrical gears.

Although existing research has extensively explored the vibration, noise, and error impacts of general gear systems, studies specifically targeting the complex dynamics of rack and pinion systems remain relatively limited. Due to the unique single-sided meshing characteristics and error accumulation effects, current literature has not sufficiently addressed the nonlinear impact of vibrations caused by the coupling of multiple error sources. While factors such as pitch errors, meshing center distance errors, and non-parallelism of axes [17] are known to affect transmission accuracy, there is a lack of in-depth analysis on how these errors interact dynamically to induce abnormal meshing states in double-idler configurations. Furthermore, few studies have proposed effective structural optimization strategies to mitigate these specific error-induced impacts. To address these gaps, this paper investigates the meshing vibration response under specific error conditions. This research not only reveals the mechanisms of error impacts on system dynamic characteristics but also proposes a flexible floating structure to optimize the stability and reliability of the system.

2. Theoretical analysis of rack and pinion meshing vibration

Similar to gear meshing, rack and pinion meshing is also a noisy transmission even under ideal conditions [18], with the main noise source being the friction noise on the tooth surface [19], which is determined by the characteristics of the involute tooth profile. In practical applications, due to the presence of an oil film, the noise generated by tooth surface friction is usually negligible [20]. However, the inevitable deformation under load, as well as manufacturing and installation errors, lead to vibrations and impacts, resulting in more intense vibration noise. Generally, gear transmission noise is divided into two categories: one is the acceleration noise caused by vibration impacts, and the other is the self-induced noise generated by the forced vibration of the gearbox [6]. Unlike gear meshing transmissions, most rack and pinion transmissions are open-type transmissions, so their main noise source is acceleration noise.

2.1. Rack and pinion meshing vibration theory

Gear meshing vibration noise is mainly caused by internal and external excitations. Internal excitations include stiffness excitation, error excitation, and friction excitation [18]. Stiffness excitation arises from the periodic variation of meshing stiffness [21]; error excitation is caused by tooth profile errors and assembly errors; friction excitation is influenced by lubrication conditions and contact characteristics [18]. External excitations are primarily caused by load fluctuations, changes in bearing support stiffness, and assembly errors. Research has been conducted on the vibration characteristics caused by the time-varying meshing stiffness of gear

racks. The following analysis mainly focuses on the vibration impact caused by error excitation.

The establishment of the dynamic model for traditional gear transmission systems is based on the lumped parameter method [22], which treats the meshing gear and rack as a vibration system with mass, spring, and damping. As shown in **Figure 1**. The vibration of this system is mainly influenced by stiffness excitation and error excitation, where stiffness excitation originates from the periodic variation of the time-varying meshing stiffness of the gear and rack, and error excitation is caused by manufacturing and assembly errors. After neglecting the elastic deformation of the gearbox, this model can effectively describe the dynamic response characteristics of the gear pair [23].

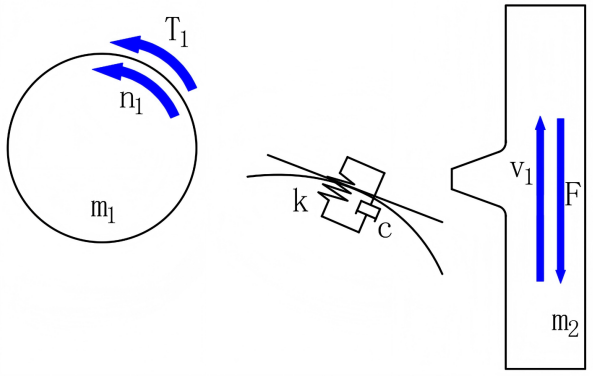

Figure 1. Mechanical model of gear rack pair.

$$M_r\ddot{X} + C\dot{X} + K(t)[X - E] = \frac{T_2}{R_1} - F \tag{1}$$

In the formula:

X—the relative displacement of the gear along the action line direction;

M_r—the equivalent mass of the gear pair;

C—the gear meshing damping;

$K(t)$—the gear meshing stiffness, which is a periodic function of time;

E—the relative displacement of the two gears along the action line direction caused by tooth deformation, errors, and faults;

T_2—the torque acting on the gear;

F—the force acting on the rack;

Since the tooth surface friction is negligible, $T_2/R_1 - F = 0$. Decompose E into two parts: E_1—the gear deformation caused by loading (zero when unloaded), E_2—the normal offset caused by errors and faults, and the time-varying meshing stiffness $K(t)$ is taken as the average meshing stiffness. Then the above equation can be simplified as:

$$M_r\ddot{X} + C\dot{X} + k_0X = k_0E_2 \tag{2}$$

A typical single-degree-of-freedom forced vibration system is constructed, where the vibration response of the gear transmission system is mainly influenced by the combined effects of damping, equivalent stiffness, and error excitation of the gear pair. Among these, the term k_0E_2, as an external excitation, reflects the impact of normal displacement caused by manufacturing errors and faults on the dynamic behavior of

the system. By introducing the average meshing stiffness k_0 and error excitation E_2, the changes in vibration characteristics caused by error excitation during the gear transmission process are analyzed.

2.2. Defect engagement analysis

In practical applications, the defective meshing errors of gear racks usually stem from rack failure and installation errors [17]. These errors cause the actual tooth profile to deviate from the ideal meshing position, disrupting the correct meshing of involute gears, leading to instantaneous transmission ratio changes, causing tooth collisions and impacts, and forming error excitation. Among the many factors influencing the vibration and noise of gear racks, pitch error and center distance error dominate, with other errors ultimately manifesting as these two types [18]. Therefore, in the field of gear rack vibration and noise research, error excitation analysis typically focuses on pitch error and center distance error. Defective meshing errors directly cause fluctuations in the instantaneous transmission ratio, leading to meshing impacts and fluctuations in meshing force, thereby becoming the main source of vibration and noise.

As shown in **Figure 2**, it is the schematic diagram of interference on single tooth engagement under the influence of pitch variation.

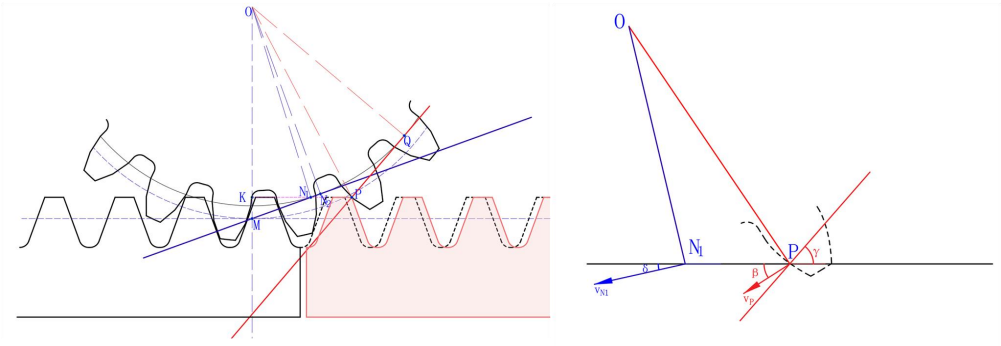

Figure 2. Offline meshing with variable rack pitch.

When the pitch of the rack changes, the engagement process that should have started at point N_1 is advanced to start at point P, At this time, the engagement angle γ at point P:

$$\gamma = \pi - arctan\left(\frac{OK}{KP}\right) - arcsin\left(\frac{OQ}{OP}\right) \tag{3}$$

Since the gear rack was installed as a standard prior to this, after entering the meshing point at P, it will slide to the point N_1 and then enter standard meshing. This sliding process is the impact process caused by pitch variation. According to the out-of-line engagement impact model [24], the direction and magnitude of the linear velocity at the actual contact point P and the theoretical meshing point N_1 undergo a sudden change, and the difference in normal velocity directly leads to the generation of normal impact load. The velocity difference Δv_{DJ} serves as a quantitative measure of the impact.

$$\Delta v_{DJ} = v_{\mathrm{P}}\, cos\left(\alpha_t - \beta\right) - v_{\mathrm{N1}}\, cos\left(\alpha_g - \delta\right) \tag{4}$$

In the formula: $v_{\mathrm{P}}, v_{\mathrm{N1}}$ are the linear velocities at the actual contact point P and

the theoretical contact point N_1 of the gear, respectively; δ is the angle between the direction of the linear velocity at the theoretical contact point N_1 and the tooth top line of the rack; β is the angle between the direction of the linear velocity at the actual contact point P and the tooth top line of the rack; the angles δ and β are calculated as follows:

$$\begin{cases} \delta = \frac{\pi}{2} - \angle ON_1K \\ \beta = \frac{\pi}{2} - \angle OPK \end{cases} \tag{5}$$

The **Figure 3** shows the interference diagram of single-tooth meshing under the influence of center distance variation.

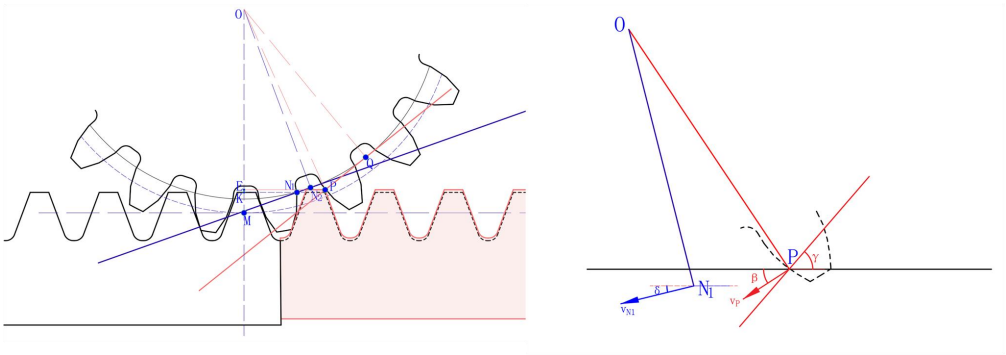

Figure 3. Off-line meshing with varying rack center distance.

When the center distance of the rack changes, the meshing process that should start at point N_1 is advanced to start at point P. At this time, the meshing angle γ at the point P is:

$$\gamma = \pi - arctan\left(\frac{OE}{EP}\right) - arcsin\left(\frac{OQ}{OP}\right) \tag{6}$$

Since the gear and rack were installed in a standard manner before this, after entering the mesh at point P, they would slide to point N_1 and then enter the standard mesh. This sliding process is the impact process caused by the change in pitch. The direction and magnitude of the linear velocity of the actual contact point P and the theoretical mesh point N_1 undergo a sudden change, and the difference in normal velocity directly leads to the generation of normal impact load.

$$\Delta v_{DZ} = v_{\mathrm{P}}\, cos\,(\alpha_t - \beta) - v_{\mathrm{N1}}\, cos\,(\alpha_g - \delta) \tag{7}$$

In the formula: $v_{\mathrm{P}}, v_{\mathrm{N1}}$ are the linear velocities at the actual contact point P and the theoretical contact point N_1, respectively; δ is the angle between the direction of the linear velocity at the theoretical contact point N_1 and the top line of the rack; β is the angle between the direction of the linear velocity at the actual contact point P and the top line of the rack; the calculation of angles δ and β is as follows:

$$\begin{cases} \delta = \frac{\pi}{2} - \angle ON_1K \\ \beta = \frac{\pi}{2} - \angle OPE \end{cases} \tag{8}$$

3. Simulation analysis of meshing under actual rack defective conditions

This chapter categorizes the error factors that significantly contribute to the vibration during the meshing process of the gears and racks in the fall arrest safety device. By analyzing the two major categories of factors—the center distance and the pitch—it explores their impact on the vibration and noise generated during the meshing process of the gears and racks in the fall arrest safety device. These factors interact to form complex vibration excitations, providing a theoretical basis for subsequent simulations and structural optimizations.

3.1. Double idler rack and pinion system construction

With the continuous increase in the lifting capacity of hoisting equipment, the working load of the safety device has also correspondingly increased. Currently, commonly used safety devices are usually equipped with two idler gears, which function by distributing the impact force generated during braking through the upper and lower teeth of the safety device gear [17], thereby reducing the bending stress at the tooth root. This design effectively prevents gear fracture caused by excessive force on a single tooth, thereby improving the smoothness and reliability of the braking process.

However, the presence of two idler gears essentially constitutes an over-constrained state. In actual operation, interference may occur between the idler gears and the rack (as shown in **Figure 4a**). To ensure that both idler gears can simultaneously engage with the rack, the center distance between the idler gears and the safety device gear must be precisely adjusted. Specifically, the distance between the two idler gears must be exactly equal to an integer multiple of the rack pitch, and the interference phenomenon can be eliminated. Additionally, to ensure the strength of the safety device gear, positive displacement treatment should be applied to the safety device gear while adjusting the center distance (as shown in **Figure 4b**). This measure ensures that the strength of the safety device gear teeth is not affected during the process of changing the center distance.

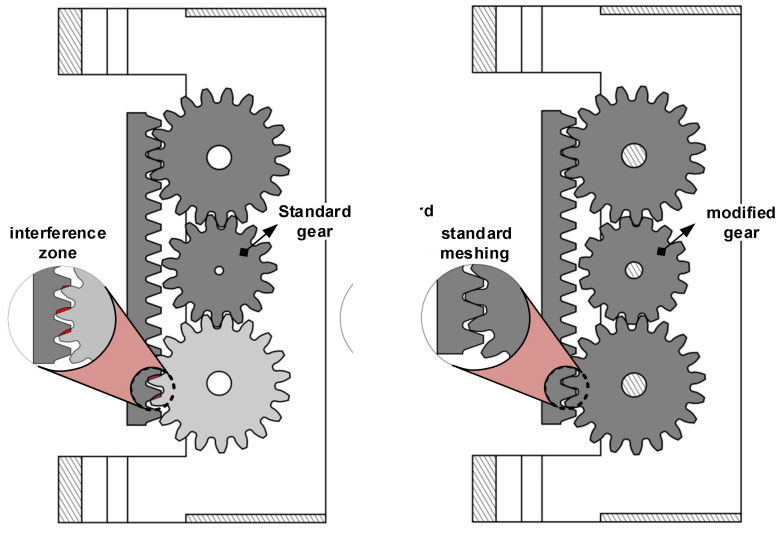

(a) Standard gear. **(b)** Modified gear.

Figure 4. The meshing interference phenomenon between the double idler and the rack.

The relevant data of the safety device gear and rack are shown in **Tables 1** and **2**:

Table 1. Gear data.

Modulus		Number of teeth	Pressure angle	Modification coefficient
safety gear	8	15	20°	0.2951
idle wheel		19		0

Table 2. Rack data.

Modulus	Pressure angle	Pitch	Top clearance coefficient	Addendum	Dedendum
8	20°	25.1327 mm	0.25	8 mm	10 mm

3.2. Defective rack and pinion construction under actual working conditions

This section aims to conduct an in-depth analysis of defective racks under two typical meshing conditions: pitch variation and center distance variation, and to construct corresponding models. Specifically, the variation in center distance mainly stems from factors such as assembly errors or rack bending damage, manifesting in two forms: sudden changes and gradual changes; while the variation in pitch encompasses sudden changes in single tooth pitch caused by gaps, as well as random minor changes in a section of rack pitch due to long-term stress deformation. To ensure the orthogonality of the experimental design, as shown in **Figure 5**, the experimental rack is divided into three sections: the two ends are standard racks, used to ensure normal meshing processes; the middle section is the experimental rack, containing the aforementioned characteristics to be studied. This sectional treatment method effectively isolates experimental variables, thereby ensuring the reliability and validity of the experimental results.

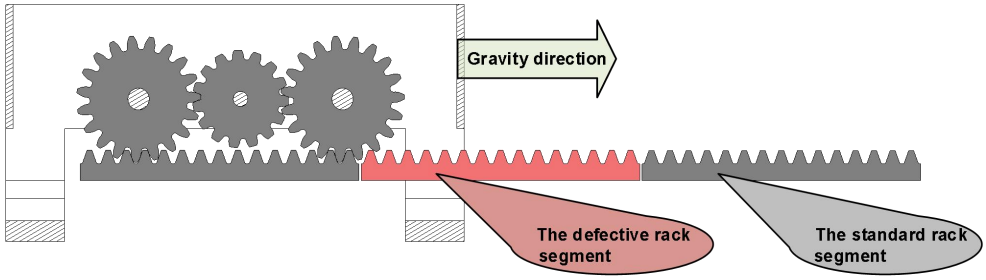

Figure 5. Experimental model layout.

3.2.1. Center distance deviation

Under the condition of defective meshing between the gear and rack, the variation in center distance primarily manifests in two forms. Firstly, due to installation errors and the bending deformation of the rack itself, there is a continuous and varying deviation between the actual center distance and the designed center distance. Secondly, during the splicing process of the rack, improper assembly at the joints may lead to a sudden change in the center distance. The combined effect of these two situations can cause the meshing center distance of the gear and rack to shift, thereby affecting

the continuity of meshing and the smoothness of transmission, ultimately leading to vibration and noise issues.

The phenomenon of sudden changes in center distance often occurs during the splicing process of the rack. When the rack is improperly assembled at the joints, it often leads to a sudden change in the center distance. As shown in **Figure 6a** of the experimental model, the installation error at the joint between two standard rack sections causes the second section to shift overall in the vertical direction, resulting in a sudden change in the center distance. The vertical coordinate in the figure represents the difference in the center distance direction between each tooth and the standard installed rack.

In contrast, during the meshing process of the gear and rack, the variation in center distance caused by installation errors and the bending deformation of the rack often exhibits a gradual nature. This deviation is manifested as a continuous change in the center distance along a section of the rack. As shown in **Figure 6b** of the experimental model, each tooth has experienced varying degrees of offset in the vertical direction, with the vertical coordinate similarly indicating the difference in the center distance direction between each tooth and the standard installed rack.

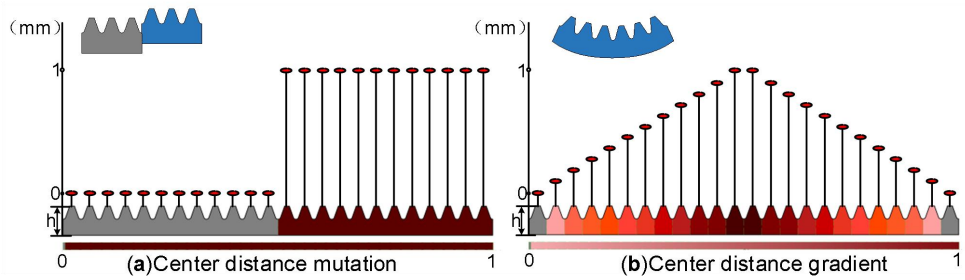

Figure 6. Rack model construction of the center distance change.

3.2.2. Pitch deviation

In the case of defective engagement of the gear and rack, the change in the rack pitch is mainly manifested in two aspects. Firstly, manufacturing defects, wear from long-term use, and overload deformation, among other factors, may cause slight changes in the pitch of a section of the rack during engagement with the gear, thereby affecting the engagement accuracy and transmission efficiency. Secondly, gaps generated during the joining of the rack can lead to pitch changes, primarily due to clearances at the joint, installation errors, or local deformation. The gaps at the joint cause sudden pitch changes at the splice of the rack, affecting transmission accuracy. With impact and wear during use, the sudden pitch change caused by the joint gap may further extend to adjacent teeth, exacerbating the uneven pitch.

The pitch changes caused by manufacturing defects, long-term wear, and overload deformation are usually small in amplitude and irregular, often randomly distributed over a section of the rack. Therefore, in the experimental model shown in **Figure 7a**, the pitch of the middle section of the rack model has been subjected to random variation. The vertical coordinate in the figure represents the difference between the pitch of two adjacent teeth and the standard pitch. For the sudden pitch changes caused by gaps, the pitch variation is characterized by a small range (typically limited to one or two teeth

at the joint) but large amplitude. The corresponding experimental model is shown in **Figure 7b**, where the joint between two standard racks causes a sudden change in pitch. The vertical coordinate in the figure represents the size of the gap.

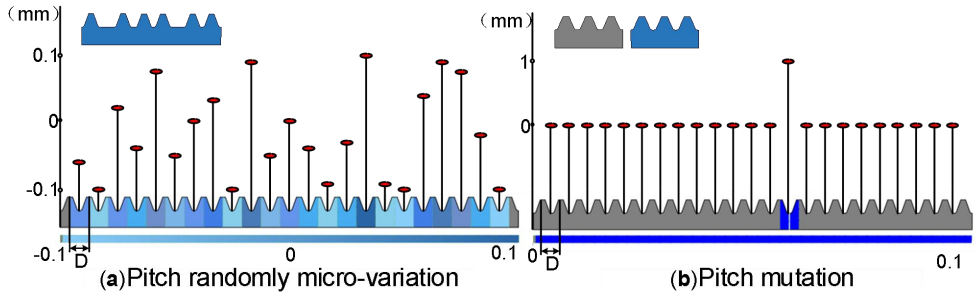

Figure 7. Pitch change rack model construction.

3.3. Analysis of defective meshing vibration under self-weight loads

Acceleration can serve as an important indicator for measuring vibration. It not only intuitively reflects the intensity of vibration but also exhibits higher sensitivity to high-frequency vibrations, capturing high-frequency components caused by instantaneous impact forces during meshing [25]. Additionally, acceleration facilitates comparative analysis with vibration test results in experiments and serves as foundational data for spectrum analysis, revealing the system's vibration frequency and resonance characteristics. This provides precise data support for subsequent vibration optimization design. This experiment employs Adams software for dynamic simulation, accurately modeling complex behaviors such as contact, friction, and deformation during gear and rack meshing, thus realistically reflecting the system's operational state.

3.3.1. Simulation pre-processing

Import the model file in STP format into Adams, assign material properties, apply revolute joints between the three gears and the housing, apply translational joints between the housing and the rack, and apply fixed joints between the rack and the ground. Select the positive direction of the x-axis as the direction of gravitational acceleration, and define the contact conditions between the two idler gears and the safety gear, as well as between the two idler gears and the rack. The load during the operation of the safety device comes only from gravity, so only a gravitational load needs to be applied to the gear mechanism. The preset simulation time is 5 s with 500 steps. After the preliminary simulation is completed, modify the simulation time to 1.5 s and the number of steps to 8000 based on the simulation results. The pre-processing setup for the simulation is now complete.

3.3.2. Simulation results and analysis

Figure 8 is the acceleration curve of the center of mass of the shell along the gravity direction extracted from the post-processing interface of the simulation.

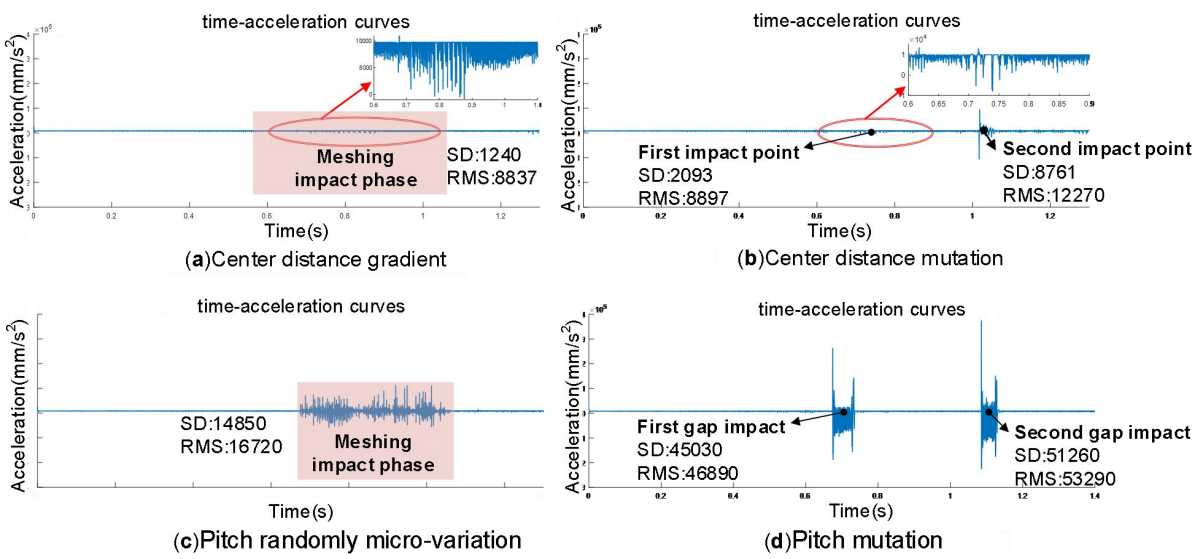

Figure 8. Shell acceleration time domain diagram.

According to the amplitude of acceleration, the influence of gaps on pitch variation is relatively significant, with a larger amplitude. Continuous minor pitch variations also cause noticeable acceleration fluctuations, though the amplitude is smaller compared to the impact of gaps. For changes in center distance, constant center distance variations do not result in significant acceleration changes. However, the center distance changes caused by joints are positively correlated with speed. The acceleration change caused by the first gap is smaller, while the second segment is more pronounced.

3.3.3. Vibration analysis

The vibration condition of a structure can be measured by the vibration severity of the structure. Vibration intensity can be quantitatively described by the root mean square values of structural vibration displacement, vibration velocity, or vibration acceleration [25]. In engineering, the root mean square of vibration velocity is commonly used to quantitatively describe vibration intensity, and its mathematical definition is:

$$V_s = \sqrt{\left(\frac{\sum V_x}{N_x}\right)^2 + \left(\frac{\sum V_y}{N_y}\right)^2 + \left(\frac{\sum V_z}{N_z}\right)^2} \tag{9}$$

In the equation, $V_s$represents the vibration severity described by vibration velocity, with the unit of mm/s; N_x, N_y, N_z are the number of measurement points in the three mutually perpendicular directions of x , y, z respectively; V_x, V_y, V_z are the root mean square values of structural vibration velocity in the three mutually perpendicular directions of x , y, z , and the corresponding calculation expressions for each direction are:

$$V_{rms} = \sqrt{\frac{1}{T}\int_0^T V^2(t)dt} \tag{10}$$

In the formula, V_{rms} is the root mean square value of vibration velocity, with the unit of mm/s; $V\ (t)$ is the function of vibration velocity varying with time, with the unit of mm/s; T is the measurement period, with the unit of s.

In order to accurately evaluate the dynamic response of the structure and obtain the nodal vibration velocity, the shell model was imported into the ANSYS Workbench transient dynamics module. To replicate the actual working conditions, as shown in **Figure 9**, fixed supports were applied to the contact surfaces of the slide rails on both sides; simultaneously, the dynamic joint loads obtained from the preceding Adams dynamic simulation were mapped onto the three intermediate shafts as time-varying boundary excitations [26].

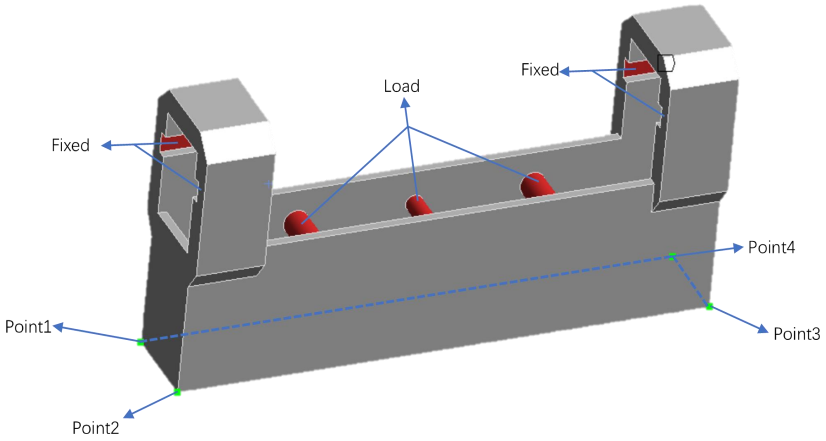

Figure 9. Vibration finite element.

Consequently, the vibration velocity data of the shell was obtained, as shown in **Figure 10**. To quantify the vibration intensity, four characteristic nodes (**Figure 9**) at the top were selected as monitoring points to extract the response curves. **Figure 11** presents the corresponding mesh quality statistics and force convergence residual plot. The discretized model consists of 193,507 nodes and 42,589 elements, predominantly composed of high-quality Hex20 units. These metrics indicate that the model exhibits good convergence and high mesh quality.

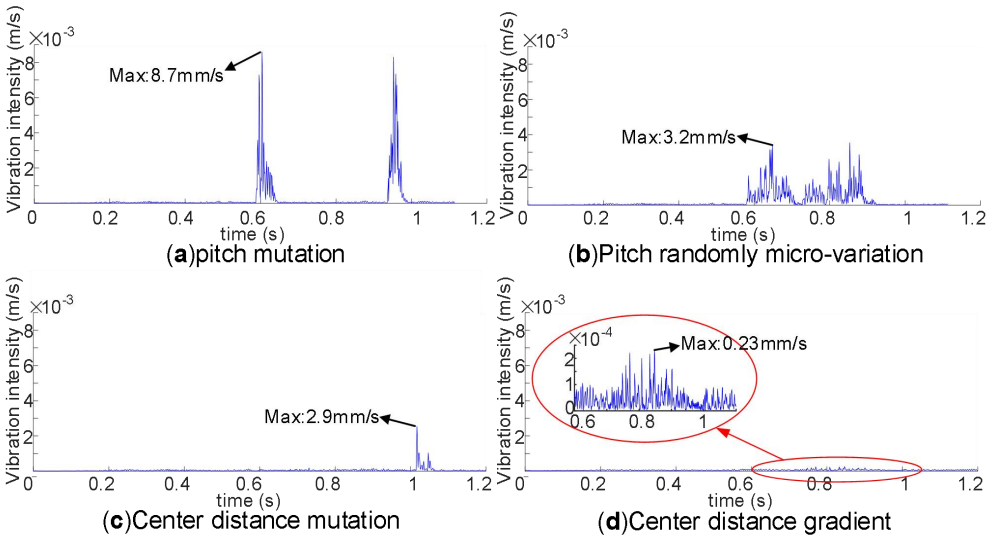

Figure 10. Time-domain plot of vibration intensity.

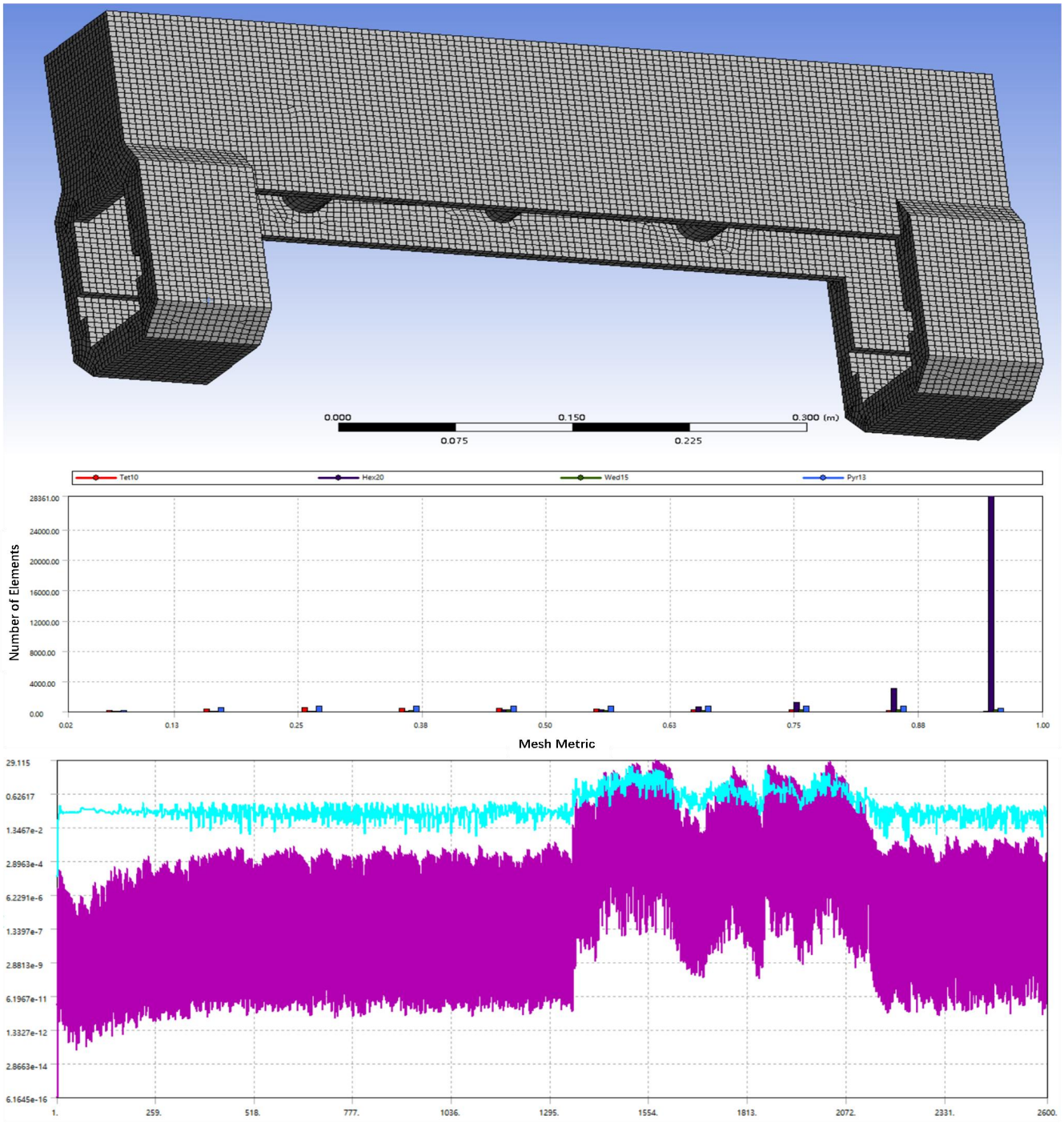

Figure 11. Mesh Quality Statistics and Model.

From these four time-domain plots, it can be observed that different error conditions exhibit distinct impact patterns in the vibration response: when the center distance changes abruptly, a pronounced and steep impact peak appears in the latter half, demonstrating a strong instantaneous acceleration pulse; gradual center distance variation induces relatively mild but prolonged vibration fluctuations; when pitch mutation occurs due to gaps, the meshing process generates sudden large pulses at specific moments, with higher and concentrated peaks; whereas random minor pitch variations scatter multiple small-to-medium amplitude peaks throughout the time domain, forming a dispersed vibration feedback. The sensitivity of defective meshing

between double idlers and the rack to pitch variation is significantly higher than that to center distance changes.

4. Comparison of improvement programs and vibration data

This chapter focuses on the structural optimization of the gear-rack meshing mechanism, with an emphasis on improving vibration and noise issues caused by installation errors and long-term use. In actual working conditions, the meshing state between the gear and rack often deviates from the designed state due to insufficient installation accuracy and accumulated wear during use, leading to additional off-line meshing impact forces, which in turn cause vibrations and noise, affecting the stability and service life of the system's transmission. The structural optimization scheme proposed in this chapter adopts a floating gear structure, where a mechanism similar to a cross slider is installed on the gear shaft of one side idler, allowing the gear shaft to have two degrees of freedom in a plane perpendicular to the axis. Flexible constraints are provided by springs, enabling automatic adjustment and compensation for deviations caused by installation errors and wear. This improvement can effectively reduce the impact forces under non-ideal meshing conditions, enhance contact quality, and thereby achieve a reduction in vibration and noise. Through Adams dynamics simulation verification, this optimization solution demonstrates significant advantages in improving transmission dynamic performance and extending equipment service life.

4.1. Improvement program and modeling

The core of the design lies in the adoption of a floating gear structure. By installing a mechanism similar to a cross slider on the idler gear shaft on one side, the gear shaft gains two degrees of freedom within a plane perpendicular to its axis, enabling adaptive fine-tuning during the meshing process. The cross slider mechanism allows the gear shaft to independently adjust its position in both horizontal and vertical directions, compensating for pitch deviations and center distance changes caused by imprecise installation and cumulative rack wear. This compensation effectively reduces the additional off-line meshing impact force introduced by pitch deviations at the seam of the gear rack, thereby improving the dynamic performance of the entire meshing process.

In structural design, the cross-slider mechanism employs a spring as a flexible constraint element, as shown in **Figure 12**, whose role is to provide appropriate feedback force for the gear shaft, enabling it to quickly buffer and return to the ideal position when subjected to impact. Simultaneously, by reasonably designing the geometric dimensions, travel range, and constraint torque of the slider, it ensures that the meshing state of the gear and rack remains stable under normal operating conditions. When affected by installation errors or wear, the mechanism can automatically adjust, reducing impact and vibration.

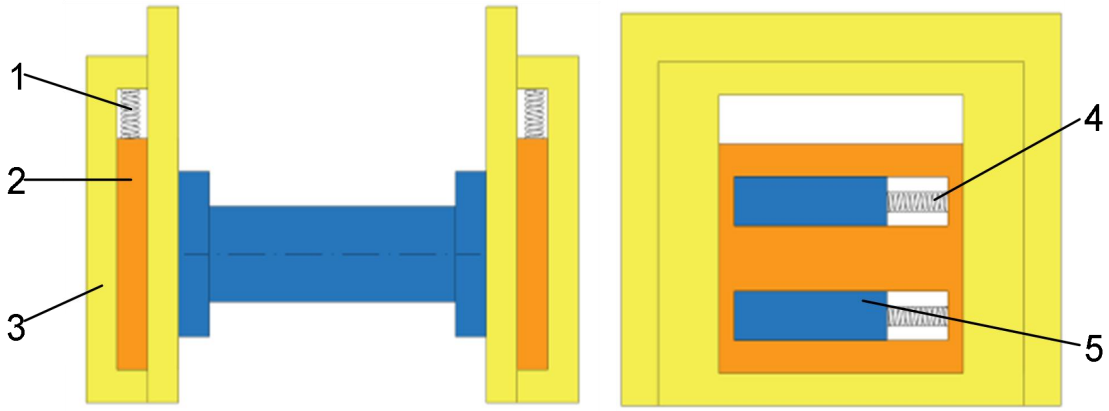

Figure 12. Enhanced floating gear shaft structure.

Note: 1—longitudinal jogging spring; 2—longitudinal floating slider; 3—Fixture; 4—transverse jogging spring; 5—transverse floating slider.

4.2. Comparison of simulation data under the same operating conditions

By quantitatively comparing the vibration acceleration response of the improved floating gear structure with the traditional rigid design, the actual effectiveness of structural optimization measures is systematically evaluated. Using the Adams simulation platform, gravity-direction acceleration loads are applied under standard working conditions to simulate the dynamic responses under four different working conditions. By contrasting the peak acceleration values and their spectral characteristics of the improved scheme under various impact conditions, the advantages of the enhanced structure in mitigating additional impact forces caused by installation errors and usage wear are thoroughly explored.

As shown in **Figure 13** by comparing the vibration time-domain diagrams of the original mechanism and the improved mechanism under four error conditions, it is evident that the improved structure has significant advantages in mitigating vibrations: under the condition of pitch mutation caused by gap issues, the improved structure effectively reduces the instantaneous impact peak and significantly decreases severe vibrations; in the condition of random pitch micro-variation, the original mechanism frequently exhibits medium to high amplitude acceleration pulses, while the improved structure makes the acceleration response more stable and greatly reduces the peak value; under the condition of center distance mutation, the improved design significantly reduces the impact force generated during the mutation; and in the condition of gradual center distance change, the improved mechanism, through an adaptive adjustment mechanism, stabilizes the overall vibration amplitude, avoiding prolonged high vibrations caused by error accumulation. Overall, the structural optimization of the floating gear and flexible support effectively reduces acceleration impacts caused by various errors, enhancing the stability and vibration resistance of the rack and pinion transmission system.

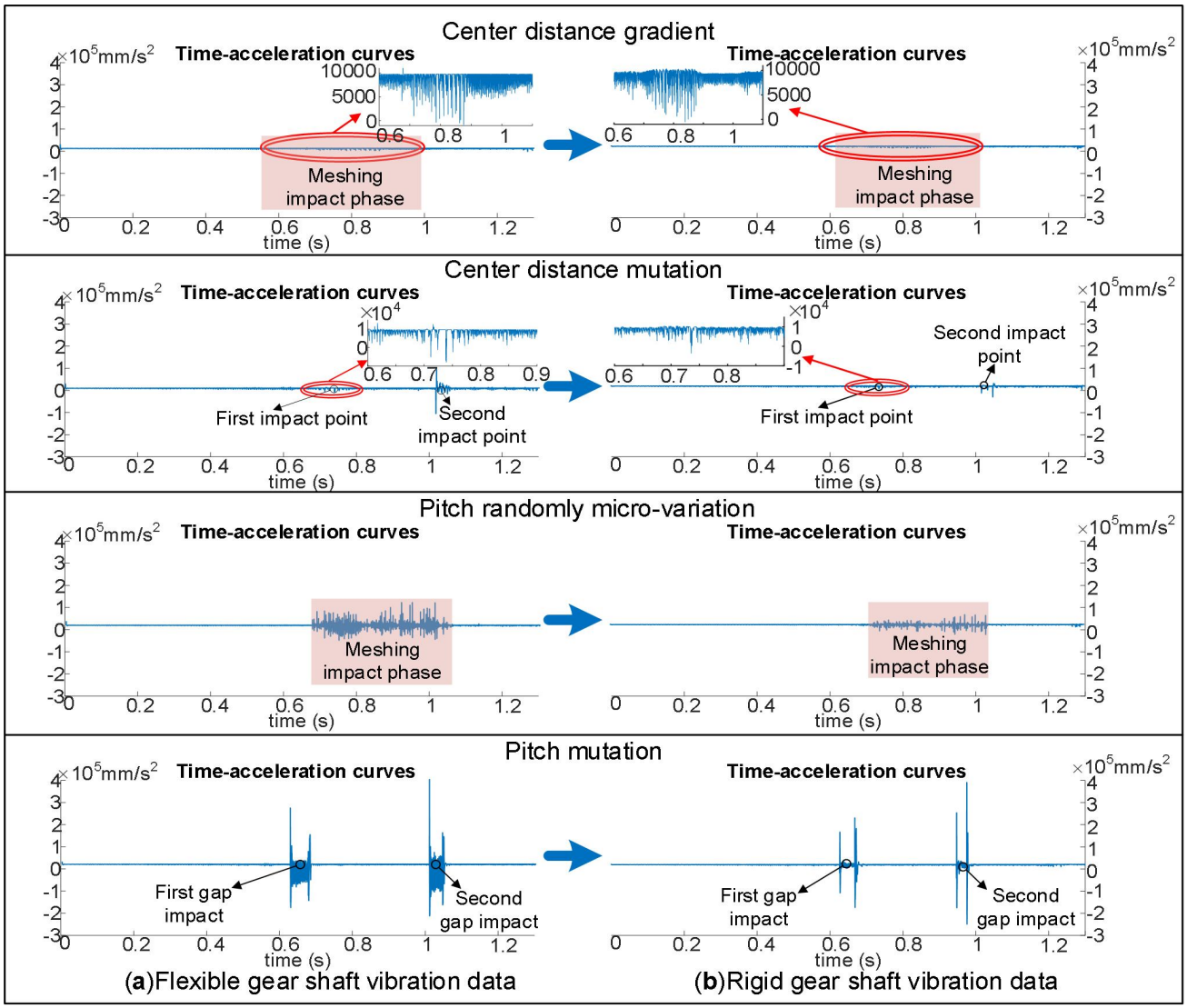

Figure 13. Post-Improvement vibration data comparison.

5. Conclusion

In this paper, the out-of-line meshing of gears and racks caused by different types of errors is classified, and the influence of different types of out-of-line meshing on meshing vibration is analyzed theoretically. Then, the dynamic simulation experiments are carried out for different out-of-line meshing conditions, and the acceleration is used as the quantitative standard of vibration intensity. Finally, the original structure is improved to reduce the impact. The specific results are as follows:

1. For the two types of out-of-line meshing in the center distance direction and the pitch direction, the influence of out-of-line meshing in the pitch direction on the meshing vibration is much greater than that in the center distance direction.
2. For the offline meshing with varying center distance direction, the vibration effect of the center distance increasing process is larger than that of the center distance decreasing process. For offline meshing in the pitch direction, due to the over-constrained nature of the double-idler mechanism, the influence of pitch defect errors on the meshing mechanism is not limited to gear engagement. Vibration impacts occur throughout the entire process as the double-idler

mechanism passes the defect, and due to the cumulative effect of pitch errors, even minor pitch variations can lead to significant vibration impacts.

3. Replacing the rigid gear shaft with a flexible floating gear shaft effectively mitigates the impacts caused by off-line meshing. Given that vibrations are highly sensitive to pitch variations, the improvement provided by the flexible shaft is particularly significant in this regard. As illustrated in **Figure 14**, the effective vibration values decreased by 60.5% and 23.4% for random pitch micro-variations and sudden rack pitch changes, respectively. Meanwhile, reductions of 57.01% and 5.3% were observed for sudden and gradual changes in the rack center distance.

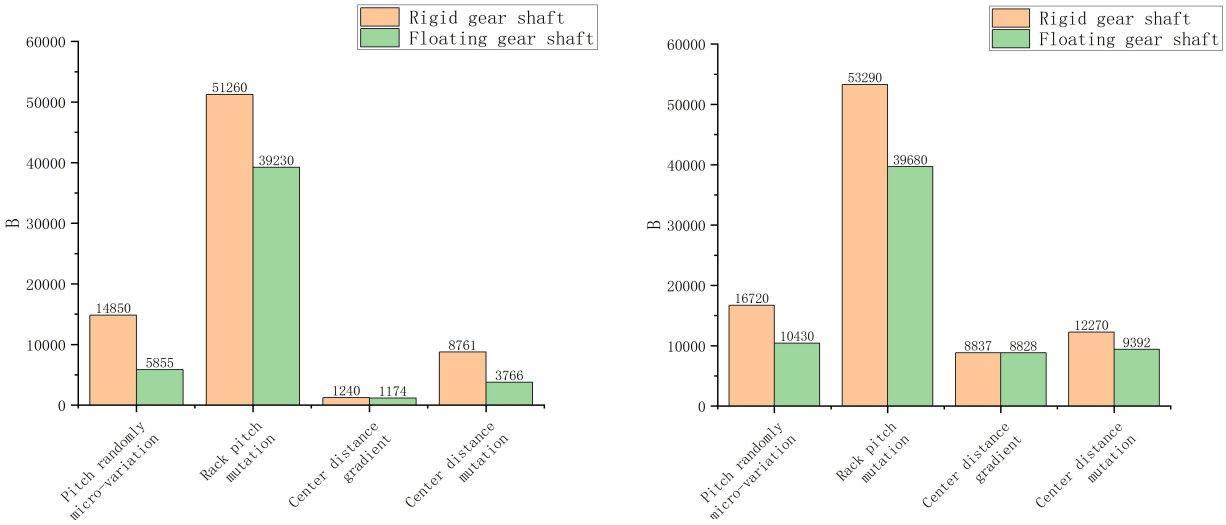

(a) Standard deviation of vibration acceleration. **(b)** RMS of vibration acceleration.

Figure 14. Improved comparative analysis of mechanical vibration data.

Author contributions: Conceptualization, PW and SG; methodology, WH; software, PW and WH; validation, PW, WH and SW; formal analysis, CR; investigation, SG; resources, JY; data curation, PW; writing—original draft preparation, PW; writing—review and editing, SW and WH; visualization, PW; supervision, WH; project administration, SW; funding acquisition, WH. All authors have read and agreed to the published version of the manuscript.

Funding: This research received no external funding.

Institutional review board statement: Not applicable.

Informed consent statement: Not applicable.

Data availability statement: The data presented in this study are available on request from the corresponding author.

Acknowledgment: The authors would like to thank the experimental team for their support and assistance with this study.

Conflict of interest: The authors declare no conflict of interest.

References

1. Mélot A, Perret-Liaudet J, Rigaud E. Vibro-impact dynamics of large-scale geared systems. Nonlinear Dynamics. 2023; 111(6): 4959–4976. doi: 10.1007/s11071-022-08144-5
2. Sun X, Zhang R, Wang Z, et al. Investigation of Spur Gear Dynamics with Gear Mesh Impacts Induced by Tooth Wear. Journal of Physics: Conference Series. 2022; 2184(1): 012039. doi: 10.1088/1742-6596/2184/1/012039
3. Zhang J, Sui W, Dhupia J. A Simplified Formulation to Estimate Influence of Gearbox Parameters on the Rattle Noise. Sound & Vibration. 2019; 53(2): 38–49. doi: 10.32604/sv.2019.04362
4. Liao L, Xiao B, Huang K, et al. A New Diagnostic Method Applied to Gearbox Missing Gear Faults ——LOD-ICA. Energy Engineering. 2022; 119(3): 1219–1238. doi: 10.32604/ee.2022.017471
5. Han H, Yuan K, Ma H, et al. Mesh characteristic analysis and dynamic simulation of spur gear pair considering corner contact and tooth broken fault. Engineering Failure Analysis. 2023; 143: 106883. doi: 10.1016/j.engfailanal.2022.106883
6. Tong S, Cheng W, Tong Z, et al. Tooth impact noise modeling of light-loaded gears under elasto-hydrodynamic lubrication: A numerical and experiment study. Applied Acoustics. 2025; 239: 110814. doi: 10.1016/j.apacoust.2025.110814
7. Xiong Y, Wang M, Huang K, et al. Research on friction and meshing efficiency of ADC12-POM gear pair considering off-line meshing. Tribology International. 2024; 200: 110116. doi: 10.1016/j.triboint.2024.110116
8. Imin R, Geni M. Stress Analysis of Gear Meshing Impact Based on SPH Method. Mathematical Problems in Engineering. 2014; 2014(1): 328216. doi: 10.1155/2014/328216
9. Ning J, Chen Z, Chen Z, et al. Dynamic behaviours of rack vehicle-track system considering rack flexibility under gear-rack mesh impact. International Journal of Rail Transportation. 2025; 13(3): 490–510. doi: 10.1080/23248378.2024.2357628
10. Yang G, Chen Z, Chen Z, et al. Dynamic investigation of a rack vehicle–track coupled system considering effect of multi-stage gear transmissions. Nonlinear Dynamics. 2025; 113(9): 9509–9528. doi: 10.1007/s11071-024-10607-w
11. Zhu LY, Yang WJ, Gou XF, et al. Dynamic characteristics of spur gear pair considering meshing impact and multi-state meshing. Meccanica. 2023; 58(4): 619–642. doi: 10.1007/s11012-023-01640-x
12. Geng Z, Chen M, Wang Y, et al. New Multi-Channel VSMFxLMS Algorithm for Vibration Reduction of Gear Systems. Chinese Journal of Mechanical Engineering. 2024; 37(1): 115. doi: 10.1186/s10033-024-01112-7
13. Liu Y, Hong T, Li Z. Influence of Toothed Rail Parameters on Impact Vibration Meshing of Mountainous Self-Propelled Electric Monorail Transporter. Sensors. 2020; 20(20): 5880. doi: 10.3390/s20205880
14. Ma H, Wang J, Han B, et al. Nonlinear fast kurtogram for the extraction of gear fault features with shock interference. Measurement Science and Technology. 2023; 34(2): 024001. doi: 10.1088/1361-6501/ac97fd
15. Dai X, Cooley CG, Parker RG. An Efficient Hybrid Analytical-Computational Method for Nonlinear Vibration of Spur Gear Pairs. Journal of Vibration and Acoustics. 2019; 141(1): 011006. doi: 10.1115/1.4040674
16. Wang F, Xu X, Fang Z, et al. Study of the influence mechanism of pitch deviation on cylindrical helical gear meshing stiffness and vibration noise. Advances in Mechanical Engineering. 2017; 9(9): 168781401772058. doi: 10.1177/1687814017720586
17. He Q, Yang G, Bao H, et al. Noise reduction measures for construction lift with idler security. Construction Mechanization. 2012; 33(5): 42–43. (in Chinese)
18. Wang B. Low Noise Gear Manufacturing Technology. Wuhan University Press; 2018. (in Chinese)
19. Li Wen, Wang L, Chang S, et al. Tooth friction bending effect of helical gear on gear dynamics. Journal of Ship Mechanics. 2013; 17(8): 937–943. (in Chinese)
20. Liu G, Nan M, Liu L, et al. A review on tribodynamics and friction noise of gears. Journal of Vibration and Shock. 2018; 37(4): 35–41. (in Chinese)
21. Ulacia I, Sánchez MB, Iñurritegui A, et al. Theoretical analysis of transmission error in rack and pinion systems. MATEC Web of Conferences. 2023; 387: 01001. doi: 10.1051/matecconf/202338701001
22. Meng Z, Shi G, Wang F. Vibration response and fault characteristics analysis of gear based on time-varying mesh stiffness. Mechanism and Machine Theory. 2020; 148: 103786. doi: 10.1016/j.mechmachtheory.2020.103786
23. Zhou Y, Shi X, Guo D, et al. Nonlinear dynamic behaviour and severity of lightly loaded gear rattle under different vibro-impact models and internal excitations. Nonlinear Dynamics. 2024; 112(2): 961–993. doi: 10.1007/s11071-023-09113-2

24. Zhou CJ. Research on the Calculation Method of Gear Bending Strength and Tooth Surface Friction Coefficient under Various Loads [PhD Thesis]. Hunan University; 2013. (in Chinese)
25. Li S, Zhang Q, Li L, et al. Analysis and Research on Vibration Severity of Planetary Shifting Mechanism. IOP Conference Series: Materials Science and Engineering. 2020; 782(5): 052007. doi: 10.1088/1757-899X/782/5/052007
26. Dadon I, Koren N, Klein R, et al. A realistic dynamic model for gear fault diagnosis. Engineering Failure Analysis. 2018; 84: 77–100. doi: 10.1016/j.engfailanal.2017.10.012